Potent 2,2-Diphenyl-1-picrylhydrazyl Radical-Scavenging Activity of Novel Antioxidants, Double-Stranded Tyrosine Residues Conjugating Pyrocatechol

Shigeki KOBAYASHI,*[,a] Tsukasa WAKI,[a] Ikuo NAKANISHI,[b] Ken-ichiro MATSUMOTO,[b] and Kazunori ANZAI[b]

[a] *Division of Analytical Chemistry of Medicines, Showa Pharmaceutical University; 3–3165 Higashitamagawagakuen, Machida, Tokyo 194–8543, Japan: and* [b] *Radiation Modifier Research Team, Heavy-Ion Radiobiology Research Group, Research Center for Charged Particle Therapy, National Institute of Radiological Sciences; 4–9–1 Anagawa, Inage-ku, Chiba 263–8555, Japan.* Received May 4, 2010; accepted August 23, 2010; published online August 30, 2010

New potent antioxidants conjugating the catechol (=pyrocatechol; pyrCat) group to two N-termini of modified double-stranded tyrosine residues were synthesized and showed radical scavenging activity with 2,2-diphenyl-1-picrylhydrazyl radical (DPPH radical, DPPH˙) as a free radical model, second-order rate constants for the DPPH˙ scavenging reaction, and the results from electron spin resonance (ESR) studies. It was found that the tyrosine (Tyr) residue and pyrCat containing new antioxidants developed in the study have about 3—20 times more potent antioxidative activity than Trolox, pyrCat, and L-ascorbic acid (VC). In order to elucidate the relationship between antioxidant activity and the molecular orbital states, and to design potent antioxidants we present an interesting approach using an absolute hardness (η)–absolute electronegativity (χ) diagram based on chemical hardness. It was shown that quantum chemicals were required to develop potent antioxidants.

Key words antioxidant; 2,2-diphenyl-1-picrylhydrazyl radical; electron spin resonance; tyrosine residue; chemical hardness

Reactive oxygen species and free radicals yielded in excess *in vivo* have been noted as a cause of the pathogenesis of various diseases, cancer, inflammation, diabetes mellitus, and neurodegenerative disease, *etc.*[1—3] Recently, it has become known that Alzheimer's disease is also caused by oxidative stress.[4,5] Free radicals yielded by the abstraction of hydrogen radical (H˙) from biological targets or one electron reduction of oxygen accumulate oxidative damage in organs *in vivo*. Organs are constantly exposed to free radicals *in vivo*, such as hydroxyl radical ˙OH, superoxide $^{\cdot}O_2^-$, singlet oxygen $^1O_2$, and others. To understand the mechanisms of oxidative damage and to design and synthesize effective antioxidants, many studies have been performed in recent years.[6,7]

Antioxidants are grouped into three main types, polyenes, polyphenols, and keto-enols, by their chemical structures and aromaticity (Fig. 1). Well-known polyenes are vitamin E (VE), licopine, and vitamin A; common polyphenols are catechins, flavonoids, catechols, and cyanidins[8]; and keto-enols are typified by L-ascorbic acid (vitamin C, VC), curcumin, and radicut (edarabon; Mitsubishi Welpharma Inc., Tokyo).[9,10] In particular, phenols, catechols, and pyrogalos are the subject of ongoing investigations because they are contained in the side chains of anthocyanins, isoflavonols, and catechins in many plant products. Their compounds are used as ligands in anticancer treatment in addition to antioxidant substances.[11]

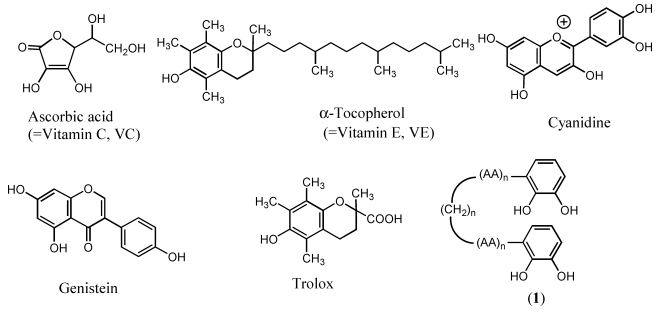

Fig. 1. Structures of Several Antioxidants and Trolox as Vitamin E Model

Theoretical investigations of molecules using chemical hardness, represented by their chemical potential (μ), electronegativity (χ) and chemical hardness (η) index,[12] are underway to characterize chemical reactions,[13,14] biological activity,[15,16] and molecular design.[17,18] To well understand the relationship between antioxidant activity and molecular hardness, we show an interesting approach using an η–χ diagram[17] for antioxidants and free radicals. Here we found that the electron states of potent antioxidants are chemically softer than $^3O_2$ and ˙OH radicals, and chemically harder than stable 2,2-diphenyl-1-picrylhydrazyl radical (DPPH˙) as a free radical model and $^1O_2$.

We aimed to design and synthesize novel antioxidants using a chemically soft catechol (=pyrocatechol, pyrCat) ligands, selected based on the chemical hardness concept.[19] The present work extends the synthesis, structure, antioxidant activity, and kinetics of novel antioxidants (**1**) conjugated with pyrCat to two N-termini of modified amino acid residues. The η values of the potent antioxidant active compound **1** are distributed to 2.23—2.34 (eV), between the values of ˙OH and DPPH˙ radicals. This may be a requirement to develop potent antioxidants.

Results and Discussion

Double-stranded tyrosines (**2a**, **b**) were synthesized using the procedures described in our previous papers.[19,20] Boc (Boc, *tert*-butoxycarbonyl)-protected tyrosine residue, Boc-L-Tyr(OBzl) was conjugated to a triethylenedioxide spacer to yield protected **2a** by the C-activating method using *N*,*N*-carbonyldiimidazole (CDI) in dry $CHCl_3$ (Chart 1). The crude compound **2a** was purified using chromatography over neu-

* To whom correspondence should be addressed. e-mail: kobayasi@ac.shoyaku.ac.jp

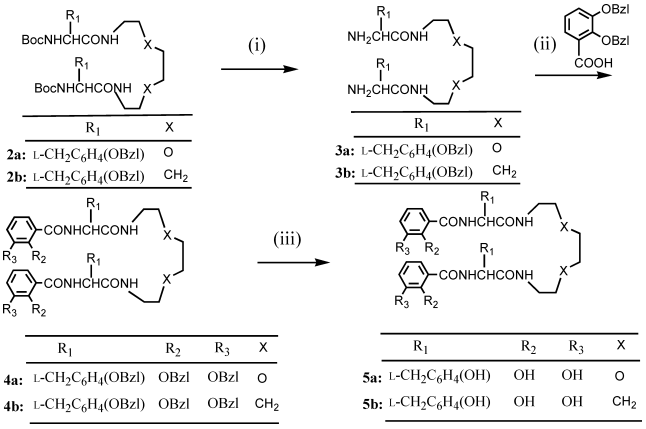

(i) 90% TFA at 4 °C. (ii) 2,3-dibenzyloxybenzoic acid, DEPC, and TEA in dry DMF at 4 °C. (iii) 5% Pd/C−H_2 in methanol.

Chart 1. Synthesis of Antioxidants **5a** and **b**

tral silica gel and the Boc-protecting group was removed by treatment with 90% trifluoroacetic acid (TFA) to produce the free form **3a**. The 2,3-dibenzyloxy benzoic acid was conjugated to **3a** to yield **4a** by the diethylphosphocyanide (DEPC) method in dry *N*,*N*-dimethylformamide (DMF). After purification of **4a**, the benzyl-protecting group of Tyr and catechols was removed with H_2 under 5% Pd–C in methanol to yield the target **5a**. Compound **5b** linked with 1,8-diaminooctane was also prepared using a similar method for **5a** in about 55% yield.

The chemical properties of novel antioxidant **1** were evaluated by measuring the ability to scavenge stable DPPH· as free radical models. To determine the antioxidative activities of **5a** and **5b**, we measured the radical-scavenging activity of **5** with DPPH·[21] as the free radical model in 90% ethanol. Antioxidant activities are obtained from the slope of the plot of [DPPH·] *vs.* the concentration of the antioxidant. In spectral changes in the reaction of **5a** with DPPH radical, as shown in Figs. 2a and b, the maximum intensity of DPPH· at 520 nm decreased and the intensity shifted to the minimum intensity resulting from reduced $DPPH_2$ at 13 μM at 23 °C. Antioxidant activity is approximately equal to the value obtained by dividing the DPPH· concentration by the concentration of **5a** at the inflection point (Fig. 2b). As a result, the DPPH· scavenging activity of **5a** was 36.7 (Figs. 2a, b), and that of **5b** was 43.4.

On the other hand, the antioxidative activity of Trolox was 3.23. The activities of V.C and pyrCat were 2.26 and 6.0, respectively, from data using a similar method (Fig. 2). The results showed that **5a** and **5b** have about 3—20 times more potent anti-oxidative activity than Trolox, pyrCat, and VC. Antioxidant activities increased in the following order: V.C<Trolox<pyrCat≪**5a**<**5b** at 23 °C. Interestingly, we noted that DPPH· scavenging activity is related to the hydrophobicity of antioxidants and more hydrophobic **5b** is higher than **5a** and pyrCat.

Generally, DPPH· scavenging activity has been calculated using methods in the literature.[22,23] Here, we showed that a graph of $-\log([\text{antioxidant}]_i/[\text{DPPH}^\cdot]_0)$ *vs.* optical density (OD) of reaction mixtures obtained by the reaction of DPPH· with antioxidants gave an S-shaped curve, as shown in Fig. 2c. It was shown that the solution of the curve with the tangential line method is equal to the value at the inflection

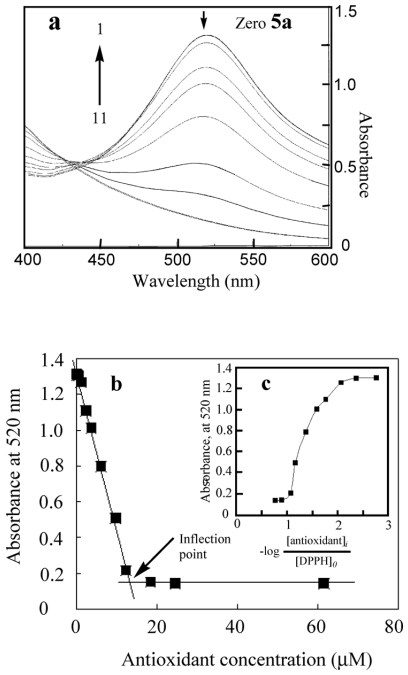

Fig. 2. Effect of **5a** on DPPH Radical Scavenging Activity

(a) Measured after reaction of DPPH· ([DPPH·]=477 μM) with 1; 0, 2; 2, 3; 5, 4; 10, 5; 20, 6; 30, 7; 50, 8; 80, 9; 100, 10; 150, and 11; 200 μl of **5a** ([**5a**]=1230 μM) in 90% ethanol for 30 min at 37 °C. (b) Plotted as a function of [**5a**] concentration. (c) Inset shows a graph plotted as $-\log$[**5a**]/[DPPH·] *vs.* absorbance.

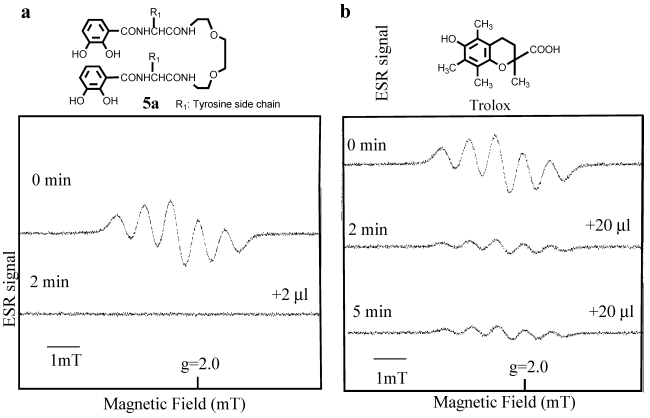

Fig. 3. Time Course of ESR Spectral Changes by Reaction of DPPH Radical with **5a** (a) or with Trolox (b)

In 90% ethanol solution of (a) [DPPH·]=383 μM, [**5a**]=4.26 μM. (b) [DPPH·]=383 μM, [Trolox]=39.8 μM.

point (Fig. 2b); therefore, the DPPH· scavenging activities are determined by Eq. 1.

$$\text{scavenging activity} = [\text{DPPH}^\cdot]_0/[\text{antioxidant}]_i \quad \text{(at the inflection point; Fig. 2b)} \tag{1}$$

Where the concentration $[\text{antioxidant}]_i$ is at the inflection point (i) in Fig. 2b. The $[\text{DPPH}^\cdot]_0$ is the concentration of DPPH· used in this experiment. Although the calculation method using Eq. 1 must be about ten titration curves, absolute values of DPPH· scavenging activities can be expressed to the second decimal.

Direct detection of the DPPH· scavenging activity of **5a** was accomplished by changes in the DPPH· signal (g=2.0061) using electron spin resonance (ESR) (Fig. 3).

The ESR spectrum of DPPH· shows quintet splitting at 0 min in 90% ethanol solution. ESR signals disappeared within 2 min by the reaction of **5a** with DPPH· (Fig. 3a); however, ESR signals of DPPH· by treatment of Trolox with DPPH· barely changed (Fig. 3b). After 5 min, the ESR signals of DPPH· had barely changed, despite treatment with 10 times concentration of Trolox against DPPH·. Obviously, the scavenging activity of compound **5a** was higher than Trolox. The changes in the ESR spectrum of **5b** provided similar results to **5a**.

To compare the dynamic antioxidant activity of synthesized **5a** with antioxidants, Trolox and pyrCat, the rapid redox reaction was analyzed using the stopped-flow spectral method (Fig. 4). Figure 4a shows stopped-flow spectral changes of DPPH· reduced by **5a** in deaerated 90% ethanol solution at 23 °C. The redox equilibrium within 2.0 s can be described as in the following Eqs. 2 and 3 (Chart 2) by the presence of one isosbestic point at 436 nm. At 27 mM DPPH·, the absorbance profiles of DPPH· at 520 nm are no longer detectable after 1.1 s, indicating that **5a** is a powerful reductant. The formation of $DPPH_2$ was also identified from the peaks of two –NH– at 8.56 and 9.06 ppm, respectively, in CD_3OD by ^{1}H-NMR. On the other hand, although pyrCat reduces oxygene O_2 to generate superoxide anion radical ($\cdot O_2^-$) in one electron transfer pathway,[24] it was found that compounds **5a** and **b** do not generate $\cdot O_2^-$ in 0.1 M KH_2PO_4 buffer (pH 7.5) (and 90% ethanol) by the chemical luminescence method (data not shown here) (Eq. 4).

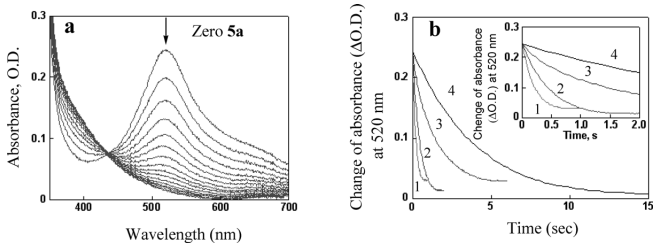

Fig. 4. Stopped-flow Spectra Recorded at 0.1 s Intervals after Mixing **5a** with DPPH· (a) and Time Changes of Absorbance at 520 nm Due to DPPH· During the Reaction with Several Antioxidants (b)

(a) [**5a**]=270 μM and [DPPH·]=27 μM. In deaerated 90% ethanol at 23 °C. (b) In the reaction of 27 μM DPPH· with (1) **5b**; 270 μM, (2) **5a**; 250 μM, (3) PyrCat; 300 μM, and (4) Troloxt; 300 μM. In deaerated 90% ethanol at 23 °C. (c) Inset shows increased time changes during 0—2 s.

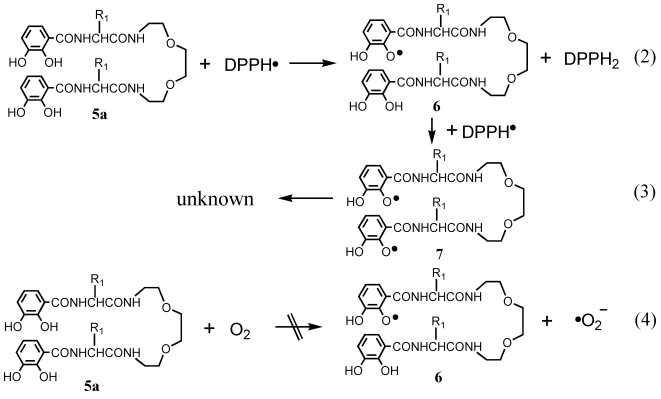

Reactions of **5a** (or **5b**) with DPPH·.

Chart 2. Possible Pathway of *o*-Semiquinones (**6** and **7**) Formation in DPPH· Scavenging

The DPPH· scavenging reactions of **5a** (or **5b**) with DPPH· *via* *o*-semiquione (**6**) and bis(*o*-semiquione) (**7**) are systematized sequentially as H· abstraction ability from **5a** (or **5b**) according to the following reactions in Eqs. 2 and 3; therefore, the autoxidation of **5a** (or **5b**) with $\cdot O_2^-$, as shown in Eq. 4, would be not expected.

Figure 4b shows the time course of the absorbance changes of DPPH· at 520 nm by the redox reaction with **5a**, Trolox, pyrCat, and **5b** in 90% ethanol. The second order rate constants (k_2) of the DPPH· scavenging of antioxidants used in this study are approximately obtained from plot of *t* (s) *vs.* ln[C]. In the condition of [antioxidant] [DPPH·], the second-order reaction rate is represented as $d[DPPH\cdot]/dt = k_{obs}[DPPH\cdot]$, where, k_{obs} is the pseudo-first-order rate constant for this kinetics step, **5a**+DPPH·→$DPPH_2$. The slope obtained from the plot of *t* (s) *vs.* ln[DPPH·] is equal to k_{obs}; therefore, k_2 gave 8.50×10^3 M$^{-1}\cdot$s^{-1} in the scavenging reaction of **5a** with DPPH· from Eq. 5.

$$k_2 = k_{obs}/[\text{antioxidant}] \quad (5)$$

The second-order rate constants of the DPPH· scavenging of **5a** and **5b** were 8500 M$^{-1}\cdot$s^{-1} and 20000 M$^{-1}\cdot$s^{-1}, resulting from the spectrum change observed during the reaction of **5a** and **5b** with DPPH·, respectively (Fig. 4b). Their scavenging rates were higher than 940 M$^{-1}\cdot$s^{-1} and 2300 M$^{-1}\cdot$s^{-1} of Trolox and pyrCat, respectively. The results clearly indicate that **5a** and **5b** have more potent antioxidant activity than pyrCat and Trolox at 23 °C, and the scavenging rates of antioxidants increased in the following order: Trolox< pyrCat≪**5a**<**5b**.

Compounds **5a** and **b** are two equivalent weights since **5a** and **b** have two catechol rings in one molecule. As a result, the ratios must be about 2 times; however, when the DPPH· scavenging activities of **5b** (or **5a**) were compared with pyrCat, the ratios were about 2.5—3.0 (=36.7/14.8—43.4/14.8) times higher against pyrCat. The ratios for DPPH· scavenging rates of **5a** were about 3.7—8.7 (=8500/2300—20000/2300) times higher than pyrCat. As an explanation, changing the electron energy, hydrophobicity and folding effect of two strands in the intramolecule as chemical properties of **5a** and **5b** are important factors to evaluate antioxidant activity. Figure 5 shows the chemical hardness[12] and the change of pyrCat, radicals and compounds **5a** and **b**. The change of electron energy is given by chemical hardness, absolute hardness (η) and electronegativity (χ).

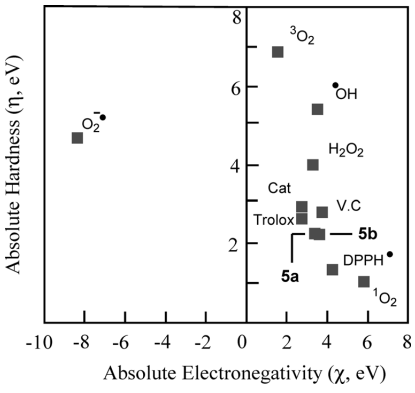

Fig. 5. A η–χ Diagram of Coordination **r**(χ, η) on the Electron State of **5a**, **5b**, DPPH·, and Reactive Oxygen Species

Table 1. Calculated Absolute Hardness (η) and Electronegativity (χ) of Reactive Oxygene Species and Antioxidants

Compounds	Absolute hardness (η), eV	Absolute electronegativity (χ), eV
Trolox[a]	2.65	2.82
VC[a]	2.76	3.76
$^3O_2$[b]	6.87	1.52
$^{\cdot}O_2^-$[b]	4.705	−8.415
H_2O_2[a]	4.005	3.335
$^{\cdot}OH$[b]	5.415	3.535
Catechol (pyrCat)[a]	2.92	2.70
$^1O_2$[b]	0.965	5.843
DPPH$^{\cdot}$[b]	1.33	4.29
5a[a]	2.239	3.47
5b[a]	2.231	3.483

a) At RB3LYP level using the 6-31G(d) basis set. *b*) At UB3LYP level using the 6-31G(d) basis set for radicals.

To elucidate the correlation between DPPH$^{\cdot}$ scavenging activity and **5a**, we computed the chemical hardness using Becke's restricted and unrestricted three-parameter nonlocal exchange and the Lee–Yang–Parr nonlocal correlation functional (B3LYP or UB3LYP) method[25] with an all-electron 6-31G(d) basis set.[26] In the molecular hardness theory, the first derivative ($-\partial E/\partial N$) is equal to electronegativity (χ), while the second derivative ($-\partial^2 E/\partial N^2$) is equal to hardness ($\eta$),[12] where E and N are the total electron energy and electron number in the system, respectively. The calculated η and χ values are listed in Table 1. Figure 5 shows the calculated η–χ diagram[17,18] as a coordinate $\mathbf{r}(\chi, \eta)$ for the electronic structures of antioxidants and radicals. The diagram shows the plot of η *vs.* χ using χ as the abscissa and η as the ordinate. From the diagram, DPPH$^{\cdot}$ and singlet oxygen ($^1O_2$) were softer free radicals than $^{\cdot}OH$ radical and triplet oxygen ($^3O_2$) in chemicals when the electronic structure coordinates of **5a** ($\mathbf{r}(3.470, 2.239)$) and **5b** ($\mathbf{r}(3.483, 2.231)$) were compared with pyrCat, Trolox, VC, and H_2O_2. We found that the magnitude of η increased in the following order: DPPH$^{\cdot}$<**5b**<**5a**<Trolox<VC<pyrCat<H_2O_2<$^{\cdot}O_2^-$<$^{\cdot}OH$<$^3O_2$. It is apparent that these orders are equal to the intensity of the radical scavenging activity between DPPH$^{\cdot}$ and antioxidants such as **5a** and Trolox. In addition, the diagram suggests that H radical abstraction from H–O–O–H does not easily occur by DPPH$^{\cdot}$.

In fact, the scavenging activity of H_2O_2 by DPPH$^{\cdot}$ is lower than Trolox and VC. Our results show that softer compounds containing phenol or polyphenol groups in the molecule provide more potent DPPH$^{\cdot}$ scavenging activity; therefore, it is a useful guideline to design and develop effective antioxidants using the η–χ diagram. Powerful antioxidants are chemically soft compounds.

Conclusion

We reported the synthesis and potent antioxidant properties of novel double-stranded tyrosine chelators **5a** and **5b** conjugated with pyrCat. According to the results of DPPH$^{\cdot}$ scavenging activity using UV/Vis titration and the stopped-flow spectral method, **5a** and **5b** are more active than pyrCat, Trolox, VC, and H_2O_2. Antioxidant activities may be estimated by the product of both static DPPH$^{\cdot}$ scavenging activity and dynamic scavenging rates. Moreover, antioxidant activities are related to chemical hardness, the potency of which can be estimated using the η–χ diagram as a coordinate $\mathbf{r}(\chi, \eta)$ of the electron structure in antioxidants. Potent antioxidants have two requirements for their molecular design: (i) absolute hardness is softer than OH radical, H_2O_2, or $^{\cdot}O_2^-$ and (ii) harder than DPPH$^{\cdot}$ or $^1O_2$. The potent antioxidants, **5a** and **5b**, presented in this study satisfy these two requirements for molecular hardness. Rather, we have reported that compounds **5a** and **5b** are applicable to the inhibitors of Alzheimer's disease-related β-amyloid protein aggregation[27] and chelators.[19] The antioxidant activities of **5a** and **5b** may provide useful pharmacological properties as model compounds, such as free radical scavenging molecules.

Experimental

General Methods The melting point was determined on MP-J3 apparatus (Yanaco New Science Inc., Kyoto, Japan) and is uncorrected. Ultraviolet/visible (UV/vis) spectra were measured with a Ubest-30 spectrophotometer (JASCO Co., Tokyo, Japan). pH was measured with a pH instrument, Model HM-60G (DKK-TOA Co., Tokyo, Japan). Infrared (IR) spectra (ν_{max} in cm^{-1}) were recorded as KBr pellets on a JASCO A-102 spectrometer. Nuclear magnetic resonance (as ^{13}C-NMR and ^{1}H-NMR) spectra were obtained with a AV600 or AV300 spectrometer (Bruker Biospin K.K., Yokohama, Japan) and NMR samples were dissolved in DMSO-d_6/$CDCl_3$ (volume ratio=5 : 2) with tetramethylsilane (TMS) as an internal reference. Fast atom bombardment mass spectrometry (FAB-MS) spectral data were obtained on an LMS-HX110 spectrometer (JEOL Ltd., Tokyo, Japan), and relevant data were tabulated as *m*/*z*.

The general approach to the synthesis of the compounds (**5a** and **5b**) was described in our previous papers.[19,20] The peptide and related ligands were detected on thin-layer chromatography (TLC) plates using iodine vapor or UV absorption. Silica gel column chromatography was performed on silica gel 60N (100 mesh, neutral; Kanto Chemical Co., Tokyo, Japan). Solvent systems were as follows, A: $CHCl_3$–methanol (20 : 1), and B: $CHCl_3$–methanol (10 : 1).

Preparation of 5a DEPC (0.46 g, 2.8 mmol) was added to the solution of 2,3-bis(benzyloxy)benzoic acid (0.86 g, 2.58 mmol), **3a** (0.600 g, 0.92 mmol), and TEA (triethylamine, 0.37 ml) at 4 °C in dry DMF (20 ml). After the mixture had been stirred at 4 °C for 1 h, the resulting mixture was stirred at room temperature overnight. Ice water was added and the solution extracted several times with $CHCl_3$. The combined organic extracts were dried over anhydrous Na_2SO_4 and evaporated to dryness. The crude residue was chromatographed on silica gel (40 g) with $CHCl_3$ and 3% methanol/$CHCl_3$ (stepwise elution) as eluents. Compound **4a** was obtained as a colorless solid in about 75.0% yield; FAB-MS (nitrobenzylalchohol, NBA) *m*/*z*: 1286 ($M+H^+$).

To a solution of **4a** (1.05 g, 0.82 mmol) in methanol (80 ml) was added 5% Pd/C (0.32 g). The mixture was shaken under H_2 flow. After the reaction was completed, the catalyst was removed by filtration with a glass filter (G3–4 size). The filtrate was evaporated. The residue was dried in a vacuum to provide **5a** as a pale yellow crystal in about 55% yield; mp 122—124 °C. IR (KBr) cm^{-1}: 3300, 1650. ^{1}H-NMR (600 MHz, $CDCl_3$/DMSO-d_6) δ: 2.99 (dd, J=8.8, 13.8 Hz, 1H, βH, –C_6H_5–C<u>H</u>–), 3.08 (dd, J=5.5, 13.8 Hz, 1H, βH, –C_6H_5–C<u>H</u>–), 3.32—3.34 (m, 2H), 3.40—3.42 (m, 1H), 3.44—3.47 (m, 1H), 3.51—3.53 (m, 2H), 4.73 (ddd, J=5.5, 8.0, 8.8 Hz, 1H, –CαH–), 6.63—6.72 (m, 1H, catechol protons), 6.92—6.93 (m, 1H, Tyr protons), 6.95—7.07 (m, 1H, catechol protons), 7.25—7.26 (m, 1H, Tyr protons), 7.79 (t, 1H, J=5.5 Hz, –NHaCO–), 8.45 (m, 1H, J=7.9 Hz, –NHbCO–). ^{13}C-NMR (600 MHz, $CDCl_3$/DMSO-d_6 (5 : 2)) δ: 36.86, 38.95, 55.01, 69.25, 69.89, 114.97, 115.16, 117.69, 117.95, 118.81, 127.60, 130.10, 146.05, 149.31, 155.83, 169.32, 171.25. HR-FAB-MS (NBA) *m*/*z*: 747.2866 (Calcd for $C_{38}H_{42}N_4O_{12}+H^+$: 747.2882).

Preparation of 5b **5b** as a pale yellow crystal in about 65.7% yield; mp 151—154 °C; IR (KBr) cm^{-1}: 3330, 2920, 1640. ^{1}H-NMR (600 MHz, $CDCl_3$/DMSO-d_6) δ: 1.23 (m, 4H, oct –CH_2CH_2–), 1.42 (m, 2H, octano –CH_2–), 2.98 (dd, J=8.5, 13.8 Hz, 2H, βH, –C_6H_5–C<u>H</u>–), 3.06 (dd, 1H, J=5.6, 13.8 Hz, βH, –C_6H_5–C<u>H</u>–), 3.12 (m, 2H, –CH_2–N–), 4.70 (m, 1H, –CαH–), 6.63—6.68 (m, 2H, catechol protons), 6.92—6.93 (m, 1H, Tyr protons), 7.05—7.07 (m, 1H, catechol protons), 7.25—7.26 (m, 1H, Tyr protons), 7.65 (t, 1H, J=5.5 Hz, –NHaCO–), 8.49 (d, 1H, J=7.1 Hz, –NHbCO–). ^{13}C-NMR (600 MHz, $CDCl_3$/DMSO-d_6) δ: 26.47, 28.86, 29.05,

37.02, 39.03, 54.99 (Ca), 115.04 (catecholic C), 115.14 (catecholic C), 117.71 (aromatic C), 117.75 (aromatic C), 127.65 (aromatic C), 130.07, 146.13, 149.56, 155.83, 169.27 (amide), 170.98 (amide). HR-FAB-MS (NBA) *m/z*: 743.3290 (Calcd for $C_{40}H_{46}N_4O_{10}+H^+$: 743.3293), where compounds **5a** and **b** were stored at 4 °C.

DPPH˙ Scavenging Assay The scavenging activity of catecholated double-stranded tyrosine (**5a** and **b**) was evaluated using DPPH˙. The antioxidants and DPPH˙ were dissolved in 90% ethanol (spectrophotometric grade) at various concentrations, 360—950 μM and 129—477 μM, to prepare stock solution, respectively. An *x* ml of the antioxidant solution was mixed with 1.0 ml of 129—477 μM DPPH˙ solution in a total volume of 10.0 ml made up of 90% ethanol. After allowing the mixture to incubate for 30 min at 37 °C, the absorbance (OD) of the reaction mixture at 520 nm was measured with a spectrophotometer. For example, the concentrations of **5a** and DPPH˙ solution were 13 and 477 μM at the inflection point, respectively. Scavenging activity was 36.7 from Eq. 1. Trolox, pyrCat, and VC were used as reference samples of antioxidants **5a** and **b**. Scavenging activity was calculated using the Eq. 1. Scavenging activities were as follows: **5a**; 36.7 (=477 μM/13 μM), **5b**; 43.4 (=477 μM/11 μM), Trolox; 3.23 (=129 μM/40 μM), VC; 2.26 (=129 μM/57.1 μM), and pyrCat; 14.8 (=444 μM/30 μM).

ESR Measurements ESR (RF100 spectrometer; JEOL Ltd., Tokyo, Japan) measurements were recorded with 100 kHz field modulation operating at 9.455 GHz and in 90% ethanol solutions at 25 °C. The parameters employed were the modulation amplitude, 0.63 mT; microwave power, 2.0 mW. The *g*-values were calculated using a MnO marker as a standard.

Stopped-Flow Measurements A rapid-scan stopped-flow spectroscopic system, RSP-1000-O2NM (Unisoku Co., Ltd., Hirakata, Japan) was used. Dynamic transformation of the absorption spectra could be observed with a minimal time interval of 0.1 s after mixing the two 90% ethanol solutions at 23 °C. The spectra were recorded at 0.1 s intervals in a wavelength range of 350—700 nm under anaerobic conditions purged with N_2 gas.

Computational Chemistry Optimized conformations of antioxidants **5a** and **b** were searched using Gaussian 03 programs[26] (Gaussian, Inc., Wallingford, U.S.A.) running on an hpcs01 (HPC Systems Inc., Tokyo, Japan). The lowest energy conformers determined with conformational search (Monte-Carlo method) computation at the MMFF94 level (Spartan'08; Wavefunction, Inc., U.S.A.) was optimized using the restricted or unrestricted B3LYP level with a 6-31G(d) basis set.

Acknowledgments We thank Ms. Tamiko Kiyotani and Mr. Youichi Takase (Showa Pharmaceutical University, Tokyo) for 600 MHz NMR and FAB-MS measurements.

References and Notes

1) Dröge W., *Physiol. Rev.*, **82**, 47—95 (2002).
2) Zhou C., Huang Y., Przedborski S., *Ann. N.Y. Acad. Sci.*, **1147**, 93—104 (2008).
3) Kowluru R. A., Chan P.-S., *Exp. Diabetes Res.*, **2007**, 43603 (2007).
4) Block M. L., *BMC Neurosci.*, **9** (Suppl. 2), S8 (2008).
5) Reddy V. P., Zhu X., Perry G., Smith M. A., *J. Alzheimers Dis.*, **16**, 763—774 (2009).
6) Huvaere K., Olsen K., Skibsted L. H., *J. Org. Chem.*, **74**, 7283—7293 (2009).
7) Amorati R., Pedulli G. F., Cabrini L., Zambonin L., Landi L., *J. Agric. Food Chem.*, **54**, 2932—2937 (2006).
8) Thangapazham R. L., Passi N., Maheshwari R. K., *Cancer Biol. Ther.*, **6**, 1931—1936 (2007).
9) Wang L.-F., Zhang H.-Y., *Bioorg. Med. Chem. Lett.*, **13**, 3789—3792 (2003).
10) Watanabe T., Tanaka M., Watanabe K., Takamatu Y., Tobe H., *Yakugaku Zasshi*, **124**, 99—111 (2004).
11) Cotterchio M., Boucher B. A., Manno M., Gallinger S., Okey A., Harper P., *J. Nutr.*, **136**, 3046—3053 (2006).
12) Parr R. G., Pearson R. G., *J. Am. Chem. Soc.*, **105**, 7512—7516 (1983).
13) Tore-Labbe A., *J. Phys. Chem. A*, **103**, 4398—4403 (1999).
14) Chamorro E., Pratim K., Chattaraj P. K., Fuentealba P., *J. Phys. Chem. A*, **107**, 7068—7072 (2003).
15) Kobayashi S., Terao Y., *Chem. Pharm. Bull.*, **52**, 517—523 (2004).
16) Ishihara M., Fujisawa S., *Dent. Mater. J.*, **28**, 113—120 (2009).
17) Kobayashi S., Sameshima K., Ishii Y., Tanaka A., *Chem. Pharm. Bull.*, **43**, 1780—1790 (1995).
18) Kobayashi S., Shinohara H., Tabata K., Yamamoto N., Miyai A., *Chem. Pharm. Bull.*, **54**, 1633—1638 (2006).
19) Kobayashi S., Watanabe M., Chikuma T., *Chem. Pharm. Bull.*, **58**, 620—627 (2010).
20) Kobayashi S., Atuchi N., Wakamatsu H., Hattori M., Kawada A., Asano K., *Chem. Pharm. Bull.*, **55**, 1585—1592 (2007).
21) Blois M. S., *Nature* (London), **181**, 1199—1200 (1958).
22) From the w.w.w. site: ⟨http://antioxidant-unit.com⟩, from antioxidant unit (Tokyo), 18 March 2010.
23) Tominaga H., Kobayashi Y., Goto T., Kasemura K., Nomura M., *Yakugaku Zasshi*, **125**, 371—375 (2005).
24) Lebedev A. V., Ivanova M. V., Timoshin A. A., Ruuge E. K., *ChemPhysChem*, **8**, 1863—1869 (2007).
25) Lee C., Yang W., Parr R. G., *Phys. Rev. B*, **37**, 785—789 (1988).
26) The calculations for $^3O_2$, OH radical, H_2O_2, $^{\cdot}O_2^-$ radical, trolox, VC, $^1O_2$, DPPH˙, **5a** and **b** were carried out with the Gaussian 03 program, Revision D.02.; Frisch M. J., Trucks G. W., Schlegel H. B., Scuseria G. E., Robb M. A., Cheeseman J. R., Montgomery J. A., Vreven T. Jr., Kudin K. N., Burant J. C., Millam J. M., Iyengar S. S., Tomasi J., Barone V., Mennucci B., Cossi M., Scalmani G., Rega N., Petersson G. A., Nakatsuj H., Hada M., Ehara M., Toyota K., Fukuda R., Hasegawa J., Ishida M., Nakajima T., Honda Y., Kitao O., Nakai H., Klene M., Li X., Knox J. E., Hratchian H. P., Cross J. B., Bakken V., Adamo C., Jaramillo J., Gomperts R., Stratmann R. E., Yazyev O., Austin A. J., Cammi R., Pomelli C., Ochterski J. W., Ayala P. Y., Morokuma K., Voth G. A., Salvador P., Dannenberg J. J., Zakrzewski V. G., Dapprich S., Daniels A. D., Strain M. C., Farkas O., Malick D. K., Rabuck A. D., Raghavachari K., Foresman J. B., Ortiz J. V., Cui Q., Baboul A. G., Clifford S., Cioslowski J., Stefanov B. B., Liu G., Liashenko A., Piskorz P., Komaromi I., Martin R. L., Fox D J., Keith T., Al-Laham M. A., Peng C. Y., Nanayakkara A., Challacombe M., Gill P. M. W., Johnson B., Chen W., Wong M. W., Gonzalez C., Pople J. A., Gaussian, Inc., Wallingford CT, 2004.
27) Kobayashi S., Tanaka Y., Chikuma T., Ikeshima H., *Peptide Science*, **2009**, 235—236 (2009).